JOURNAL OF AGRICULTURAL AND FOOD CHEMISTRY

Fe_3O_4/SiO_2-*g*-PSStNa Polymer Nanocomposite Microspheres (PNCMs) from a Surface-Initiated Atom Transfer Radical Polymerization (SI-ATRP) Approach for Pectinase Immobilization

ZHONGLI LEI,* NA REN, YANLI LI, NA LI, AND BO MU

Key Laboratory of Applied Surface and Colloid Chemistry (Shaanxi Normal University), Ministry of Education, School of Chemistry and Materials Science, Xi'an 710062, China

Polymer nanocomposite microspheres (PNCMs) as solid supports can improve the efficiency of immobilized enzymes by reducing diffusional limitation as well as by increasing the surface area per mass unit. In this work, pectinase was immobilized on Fe_3O_4/SiO_2-*g*-poly(PSStNa) nanocomposite microspheres by covalent attachment. Biochemical studies showed an improved storage stability of the immobilized pectinase as well as enhanced performance at higher temperatures and over a wider pH range. The immobilized enzyme retained >50% of its initial activity over 30 days, and the optimum temperature and pH also increased to the ranges of 50−60 °C and 3.0−4.7, respectively. The kinetics of a model reaction catalyzed by the immobilized pectinase was finally investigated by the Michaelis−Menten equation. The PSStNa support presents a very simple, mild, and time-saving process for enzyme immobilization, and this strategy of immobilizing pectinase also makes use of expensive enzymes economically viable, strengthening repeated use of them as catalysts following their rapid and easy separation with a magnet.

KEYWORDS: Fe_3O_4/SiO_2 composite particles; polymer nanocomposite microspheres; enzyme immobilization

INTRODUCTION

The expanding interest in pectinase mainly lies in its wide industrial applications. Pectin has numerous applications as a functional food ingredient and is widely used as a gelling agent in the production of jams and jellies, fruit juice, confectionary products, and bakery fillings. Pectin is also used for the stabilization of acidified milk drinks and yogurts (*1*, *2*). Furthermore, pectic fragments have been shown to possess regulatory activity for plant defense mechanisms and plant development (*3*). Despite the excellent catalytic properties of pectinase, enzyme properties have to be usually improved before their implementation at industrial scale (where many cycles of high-yield processes are desired). In all cases, enzyme engineering via immobilization techniques is perfectly compatible with other chemical or biological approaches to improve enzyme functions. Enzyme industrial use could benefit from its immobilization mainly if the immobilization technique may improve its catalytic features, such as stability, activity, selectivity toward non-natural substrates, inhibition by reaction products, and facile separation from reaction mixtures (*4*−*6*). However, the final success depends on the availability of a wide battery of immobilization protocols (*6*).

Polymer nanocomposite microspheres (PNCMs) represent an attractive family of composite materials in which the nanometer-sized reinforcing fillers are uniformly dispersed in the polymer on a nanometer scale compared to conventional phase-separated macrocomposites (*7*−*9*). As one important member of inorganic nanoparticles, magnetic nanoparticles are additional important materials due to their interesting magnetic properties. Since the pioneering work developed by Ugelstad on preparation of superparamagnetic polystyrene microspheres using a so-called "activated swelling method" for immunity separation, extensive research has been carried out to develop superparamagnetic nanocomposite materials for biomedical applications. These applications include separation and purification of bimolecular, MRI contrast agent, hyperthermia, biosensor, and targeted drug delivery (*10*). Recently, Dyal et al. reported a successful method for immobilizing proteins on naked *Y*-Fe_2O_3 magnetic nanoparticles for biological use (*11*). Kouassi and Irudayaraj also developed gold-coated magnetic nanoparticles for immobilizing oligonucleotide as a DNA sensor (*12*). However, the activity of the biomolecule immobilized on these magnetic particles depends on the particular nature of the metal/oxide/hydroxide surfaces (acidity, surface coverage, and functional group uniformity). The enzyme desorbs from the particles when they are exposed to solution, suggesting that at least some of the reaction is carried out in solution and not on the surface of support. This is not the case here, where the enzymes are chemically bonded to the carrier Fe_3O_4/SiO_2-*g*-PSStNa with good biocompatibility,

* Corresponding author (e-mail zhllei@snnu.edu.cn; telephone 86 29 8530 3952; fax 86 29 8530 7774).

10.1021/jf802913m CCC: $40.75
Published on Web 01/20/2009

combining the functionality of the inorganic nanoparticles with the processability of the polymer macromolecule. More recently, polymer brush "grafting to" and "grafting from" techniques have become popular methods to modify inorganic nanoparticles (*13*−*15*).

In this work, to build more stable assembly, the polyelectrolyte brush PSStNa was grafted onto the surface of Fe_3O_4/SiO_2 composite particles by surface-initiated atom transfer radical polymerization (SI-ATRP) using modified magnetic silica as initiator. Subsequently, introducing a layer-by-layer (LbL) method, deposition occurs by electrostatic interactions between the adsorbed PSStNa and chitosan layer with opposite charges. Up to now, using the Fe_3O_4/SiO_2-*g*-PSStNa composite microsphere from the ATRP approach for pectinase immobilization has not been reported to the best of our knowledge. It was further found that Fe_3O_4/SiO_2-*g*-PSStNa nanocomposite microspheres with modified multishells enhanced the stability of both nanopaticles (compared to adsorption) in solution and the immobilized pectinase. This strategy of pectinase immobilization opens new avenues for the application of bioparticles and represents a promising route for the creation of complex catalytic particles.

MATERIALS AND METHODS

Materials. Pectin and the enzyme polygalacturonase (pectinase) were obtained from Fluka Chemical Co. (St. Louis, MO). $FeCl_3 \cdot 6H_2O$ and $FeCl_2 \cdot 4H_2O$ were purchased from Fluka. 2,2′-Bipyridine (bpy) (AR, 97.0%) provided by Beijing Chemical Co. was recrystallized twice from acetone. CuBr was purified according to a published procedure (*11*). SStNa (sodium 4-styrenesulfonate, 99%) was supplied by Fluka (New York). Chitosan was supplied by Shanghai Chemical Co. Ultrapure water (resistivity = 18.2 MX, pH 6.82) was used in all experiments. Other reagents and organic solvents for the initiator synthesis and polymerization were purchased from commercial sources.

Preparation of Polymer Nanocomposite Microsphers Fe_3O_4/SiO_2-*g*-PSStNa. This was synthesized according to our published procedure (*16*). In a typical procedure 25 wt % NH_3 H_2O) was added into the mixture of iron salts with a molar ratio ($FeCl_2/FeCl_3$) of 1:2. The reaction mixture was heated at 80 °C for 30 min, and the medium pH was maintained at 10 by the addition of aqueous ammonia solution during the reaction. The magnetite dispersion was then stirred for 1.5 h at 90 °C upon addition of a citric acid solution (0.1 M). N_2 was bubbled throughout the reaction. Subsequently, deionized water was added to wash and redisperse ultrafine magnetic particles. Then, the resultant dispersion was treated by dialysis and adjusted to 2.0 wt %. The obtained magnetite dispersion was defined as magnetic fluid (MF). Coating of magnetite nanoparticles with silica was carried out in a basic alcohol/water mixture at room temperature by using MF as seed. A suspension of the synthesized magnetic nanoparticles (1.00 g) was diluted by a mixture of ethanol (80 mL) and water (16 mL). After the addition of ammonia solution (2 mL, 25 wt %), the precursor of TEOS (1 mL) was added to the reaction solution with mechanical stirring at 25 °C for 12 h. The preformed particles were washed to eliminate excess reactants by centrifugation and dried in a vacuum oven at 70 °C.

Fe_3O_4/SiO_2/PSStNa/Chitosan Supports. The prepared Fe_3O_4/SiO_2-*g*-PSStNa colloidal particles (**Figure 1**) (0.8 g) were dispersed in 0.2 M acetate buffer of pH 3.5. A total of 2 mL of 0.5% chitosan in 1% acetic acid was added and then sonicated for 1 min. After 8 h, the excess polyelectrolyte was removed in the supernatant fraction by two centrifugation/wash/redispersion cycles. The Fe_3O_4/SiO_2/PSStNa/chitosan particles were cross-linked by treatment with 2.5% glutaraldehyde (pH 4) at room temperature for 4 h.

Enzyme Immobilization. Fe_3O_4/SiO_2/PSStNa/chitosan supports were added to the enzyme solution (8.27, 16.5, or 33 U of enzyme per milliliter of acetate buffer at pH 3.5), and the immobilization reaction was carried out in a shaking water bath for 4 h. Particles were separated, and the unbound enzymes were removed by washing three times with acetate buffer/deionized (DI) water. The immobilized enzyme was used freshly and stored at 4 °C.

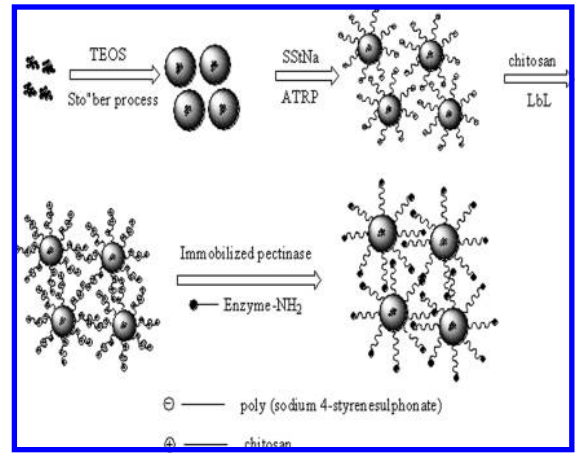

Figure 1. Schematic representation of the preparation of Fe_3O_4/SiO_2-*g*-PSStNa/chitosan particles and pectinase immobilization.

Determination of Immobilized Protein. Quantification of reducing sugars was performed according to the DNS method (*17*). The amount of reducing sugar formed was estimated by the 3,5-dinitrosalicyclic acid method (*17*). The standard compound used for the calibration curve for determining pectinase activity using 3,5-dinitrosalicylic acid is D-(+)-galacturonic acid monohydrate. Pectinase (40 mg, Fluka, St. Louis, MO) was dissolved in 1 mL of 0.2 mol/L acetate buffer at pH 4.5, added to the solutions of Fe_3O_4/SiO_2-*g*-PSStNa/chitosan particles (100 mg/ml), and stirred for 24 h at 4 °C to avoid microbial growth. The surplus of nonadsorbed enzyme was then removed by centrifugation (10000*g* for 10 min). The amount of nonadsorbed enzyme was determined from absorbance of the eluate at 520 nm (measured by using a UV−visible spectrophotometer, Shimadzu Co. Ltd., Kyoto, Japan) with the help of a calibration curve.

Pectinase Activity Assay. Pectinase activity was determined using polygalacturonic acid as a substrate (*17*). One unit of activity was defined as the amount of enzyme required to hydrolyze 1.0 mol of pectin per minute under the described conditions. The amount of reducing sugar formed was estimated according to the 3,5-dinitrosalicyclic acid method (*18*). As the polymer-linked enzyme was soluble during the assay, the activity of the immobilized preparation could be determined by following the assay procedure for the free enzyme.

Determination of Kinetic Parameters. Enzyme activities, in the free and immobilized forms, were evaluated using classical Michaelis−Menten kinetics:

$$V = \frac{V_{max}[S]}{K_m + [S]}$$

where [S] is the substrate concentration, V_{max} is the maximum reaction rate attained at infinite substrate concentration, and K_m is the Michaelis−Menten constant.

K_m and V_{max} values of native and immobilized enzyme preparations were determined by measurement of enzyme activity with various concentrations of substrate (pectic). Pectin solutions (0.05/0.1/0.2/0.4/0.6/1.0/1.5 mol/L) were prepared in 0.2 mol/L acetate buffer (pH 3.5) and kept in a water bath at 37 °C for 5 min, and then the immobilized pectinase or free enzyme solution was added to the test tubes and shaken for different incubation times. Both the free and immobilized enzyme concentrations were 1.0 mg/mL.

Determination of the Storage Stability of Free and Immobilized Pectinase. The activity of the immobilized enzyme was measured daily while standing at 4 °C for 30 days. The remaining percentage of immobilized enzyme activity was calculated in each determination.

RESULTS AND DISCUSSION

Component Analysis of Resultant Nanoparticles. The components of the resultant Fe_3O_4/SiO_2 and functionalized Fe_3O_4/SiO_2 nanoparticles as initiator were assayed by energy dispersive X-ray spectrometry (EDS) and elemental mapping

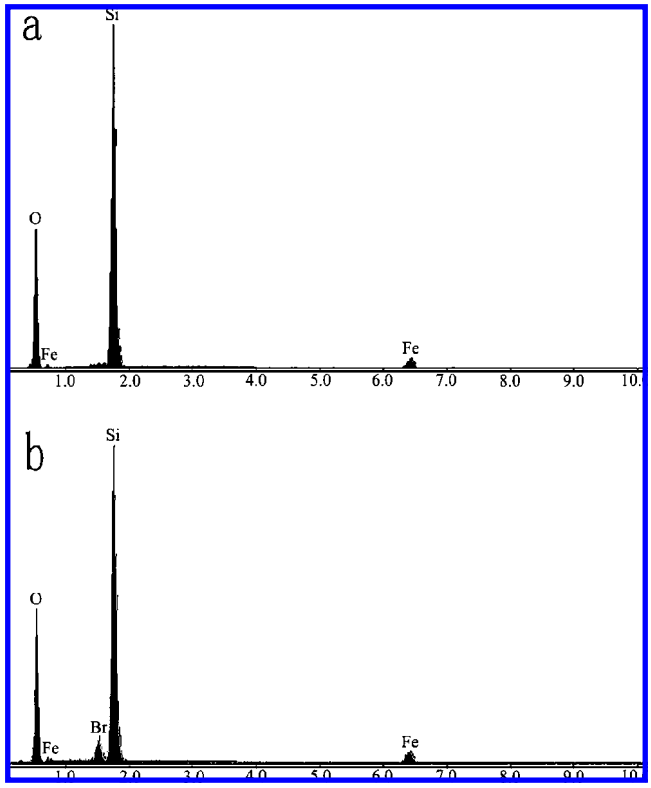

Figure 2. EDS of the (**a**) Fe_3O_4/SiO_2 particles and (**b**) initiator-modified Fe_3O_4/SiO_2.

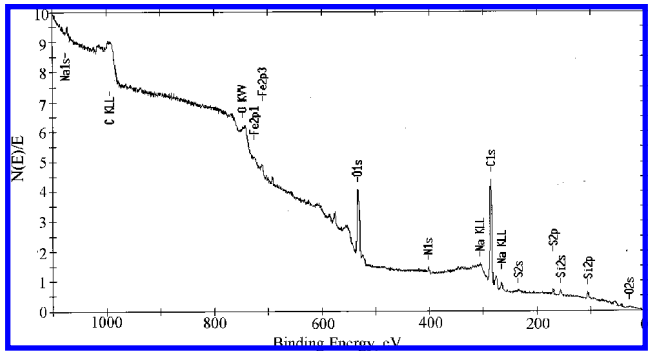

Figure 3. Survey XPS spectra of Fe_3O_4/SiO_2-*g*-PSStNa particles.

analysis. The presence of Si, O, and Fe in **Figure 2a** indicates that the iron oxide particles were loaded into silica spheres. The relatively high Si and O peaks could indicate the presence of multiple layers of SiO_2 on the surface of the Fe_3O_4 nanoparticles. The obvious characteristic peak for Br element, originating from modified Fe_3O_4/SiO_2 (**Figure 2b**) indicates that the initiators Fe_3O_4/SiO_2-Br for SI-ATRP were synthesized.

Subsequently, the chemical composition of polyelectrolyte brush poly (SStNa) being grafted onto Fe_3O_4/SiO_2 nanoparticles was analyzed using X-ray photoelectron spectroscopy (XPS) in **Figure 3**. The XPS spectra were obtained with a Sigma Probe X-ray photoelectron spectrometer (ThermoVG Scientific). The X-ray source was twin anode Al Kα radiation (1486.6 eV), and the spot size was 800 μm. Pass energies of 50 eV (for the survey spectra) and 20 eV (for the high-resolution spectra of all elements of interest) were chosen. C1*s*, N1*s*, O1*s*, Si2*p*, Fe2*p*, S2*p*, and Na1*s* spectra were detected. The characteristic peaks for C1*s*, O1*s*, Si2*p*, Fe2*p*, Na1*s*, and S2*p* were observed in the spectrum at 285, 533, 104, 701.1, 1071.5, and 167.8 eV, respectively. In addition, a weak signal at 399.2 eV, corresponding to N1*s*, was also detected. Integration of the peak areas

Table 1. XPS Surface Compositions of Fe_3O_4/SiO_2-*g*-PSStNa Particles

	element surface compositions determined by XPS (at. %)						
sample type	C1s	O1s	N1s	Si2p	Fe2p	Na1s	S2p
poly(SStNa)-*g*-Fe_3O_4/SiO_2	68.54	22.31	1.40	2.61	1.36	1.56	2.23

of the elements allowed the surface chemical composition to be calculated for each sample (see **Table 1**). As expected, poly(SStNa)-*g*-Fe_3O_4/SiO_2 particles showed the highest carbon signals, suggesting that the underlying magnetic silica substrates are partially masked by the coated polymer chains. The detection of sulfur and sodium signals is convincing evidence for the presence of poly(SStNa). A relatively weak nitrogen signal was detected for the anionic polyelectrolyte grafted Fe_3O_4/SiO_2 particles, which is probably due to bipyridine ligand impurities.

Physicochemical Structure of Resultant Support. Formation of Fe_3O_4/SiO_2-*g*-PSStNa/chitosan can be directly visualized by transmission electron microscopy (TEM), which was performed on a Philips H-600 EX transmission emission microscope operated at a 120 kV accelerating voltage. Specimens for inspection by TEM were prepared by drop-casting dilute solutions of prepared nanoparticles onto carbon-coated copper grids, followed by evaporation of the solvent in air. **Figure 4a** shows TEM images of Fe_3O_4 nanoparticles and their electron diffraction pattern, where most of the particles are quasi-spherical with an average diameter of 8 nm or so. **Figure 4b** shows TEM images of silica-coating Fe_3O_4 particles. The magnetic silica particles (MSPs) with well-defined core/shell structures were rather monodisperse, even though silica shells had trapped more than one magnetic core. The Fe_3O_4/SiO_2 particles used in this case for the production of composite microspheres had an average diameter of 70 $\pm$ 10 nm obtained by TEM images. Silica has the desirable properties of being a biocompatible, water-soluble, and nontoxic coating on the surfaces of magnetic nanoparticles; the surface properties of the magnetic nanoparticles change from hydrophobic to hydrophilic, and the magnetic dipolar attraction between magnetic nanoparticles can be screened to avoid their aggregation. In addition, the existence of a lot of silanol groups in the silica layer provides various functional groups on the surfaces of silica-coated magnetic nanoparticles. As shown in **Figure 4c**, a basic core−shell structure [dark colored core for Fe_3O_4/SiO_2 nanoparticles and light-colored shell for poly(SStNa)] was obtained, and the average increase in diameter was approximately 20 nm. Furthermore, the presence of a PSStNa shell clearly resulted in increased surface roughness. The inner iron oxide core with modified multishells stabilized more the nanoparticles in solution and avoided magnetic nanoparticles desquamating from the support during repeated use of immobilized enzyme. The magnetic properties of the support assayed in **Figure 6** also ensure facile separation of enzyme from reaction mixtures. **Figure 4d** shows TEM images of the composite nanoparticles covered with chitosan, the diameters of which increase to 120 nm and the surface of the whole composite microsphere becomes lighter than ever. In addition, the size of the polymer composite microspheres is strictly constrained in the nanoscale because nanosize composites significantly reduced the mass transfer limitation compared to other enzyme stabilization methods (*19*).

Magnetic Properties of Resultant Support. The magnetic properties of the composite microspheres were followed by a vibrating-sample magnetometer. The saturation magnetization

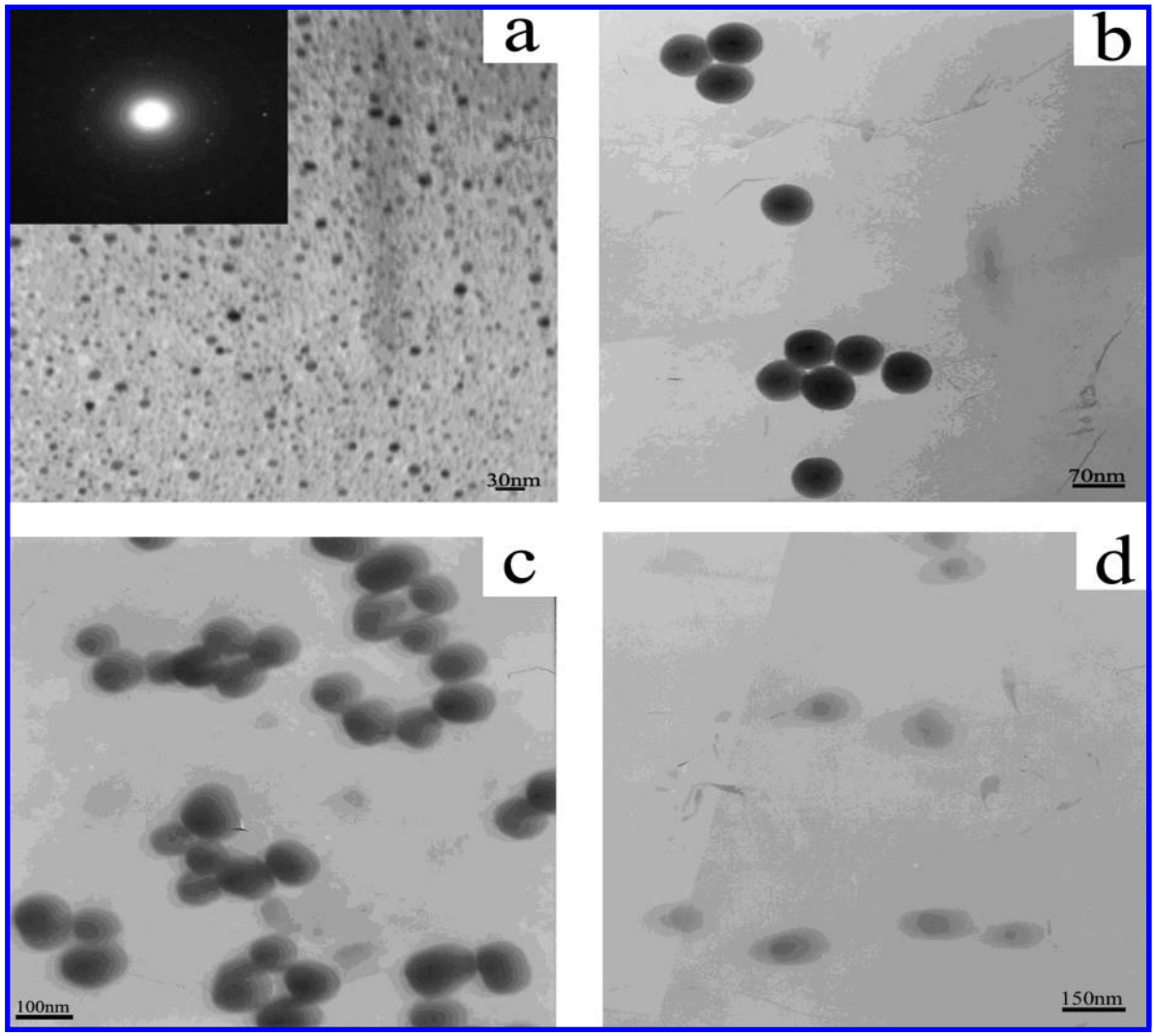

Figure 4. TEM micrographs of (**a**) Fe_3O_4 nanoparticles and their electron diffraction pattern, (**b**) Fe_3O_4/SiO_2, (**c**) $Fe_3O_4/SiO_2$2-*g*-PSStNa, and (**d**) Fe_3O_4/SiO_2/PSStNa/chitosan microspheres.

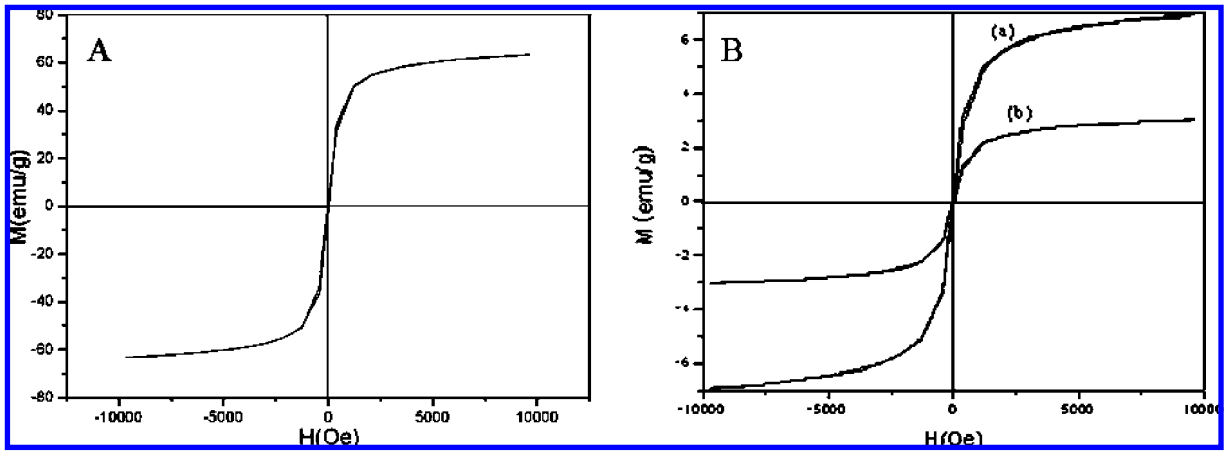

Figure 5. (**A**) Hysteresis loops of magnetite nanoparticles. (**B**) Magnetization curve of (a) Fe_3O_4/SiO_2 and (b) Fe_3O_4/SiO_2-*g*-PSStNa particles.

(M_s) of magnetite (in **Figure 5A**) reduced to 63.292 emu/g of the bulk Fe_3O_4 (92 emu/g of magnetite) (*20*). It is known that the energy of a magnetic particle in an external field is proportional to its size via the number of magnetic molecules in a single magnetic domain. This phenomenon is more significant for the nanoparticles due to their large surface to volume ratio. Therefore, it is reasonable that the saturation magnetization value for the nanoparticles is smaller compared to the bulk material.

As shown in **Figure 5B** the saturation magnetic moments of silica-coating Fe_3O_4 particles (**Figure 5B**, curve a) and polyelectrolyte-grafted Fe_3O_4/SiO_2 particles (**Figure 5B**, curve b) reached 6.9339 and 4.8154 emu/g, respectively. These low saturation magnetization values were less than the reference

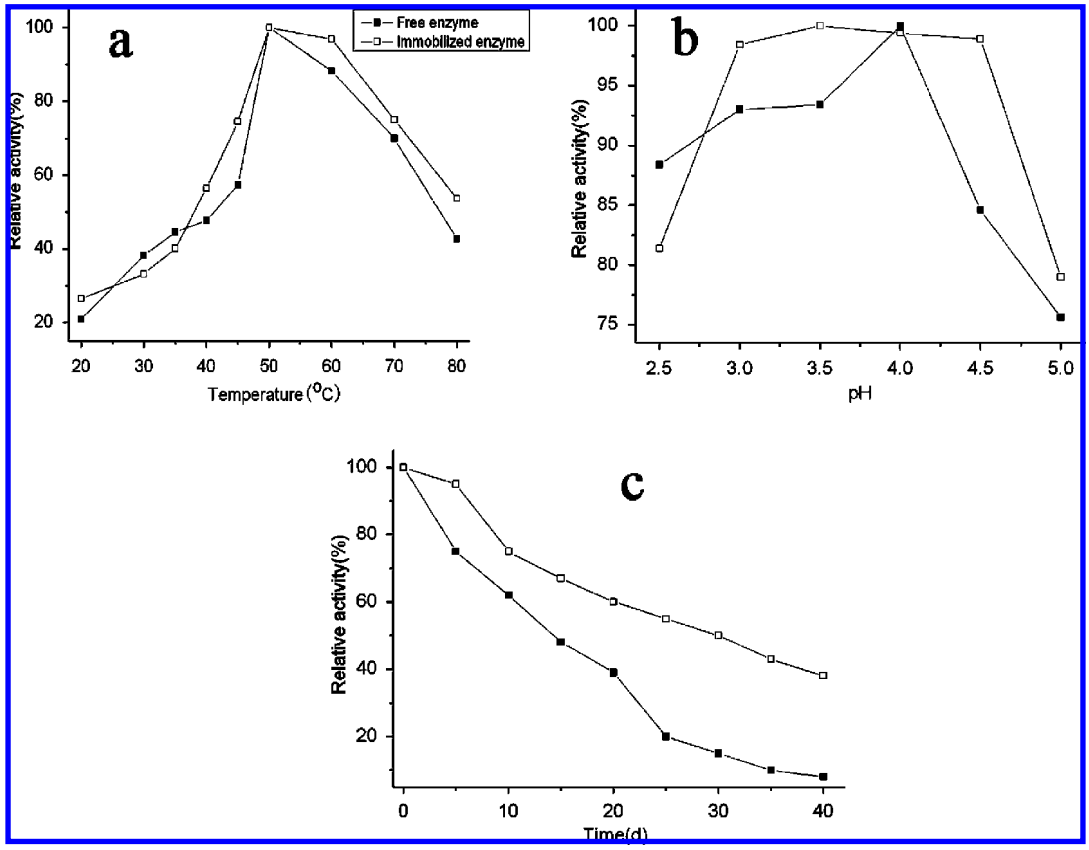

Figure 6. (**a**) Activity of free and immobilized pectinase at different temperatures: (■) free enzyme; (□) immobilized enzyme. (**b**) Activity of free and immobilized pectinase at different reaction medium pH values: (■) free enzyme; (□) immobilized enzyme. (**c**) Storage stability of immobilized enzymes: (■) free enzyme; (□) immobilized enzyme.

value for the pure magnetite nanoparticles (Fe_3O_4), which can be explained by the diamagnetic contribution of the silica shells surrounding the magnetite nanoparticles and also poly (SStNa)-grafted Fe_3O_4/SiO_2 particles weakening the magnetic moment due to the presence of polymer shells. However, both of them showed superparamagnetic behaviors, indicating that magnetic nanoparticles exhibited no remaining effect from the hysteresis loops at the applied magnetic field. One of the main goals of immobilizing enzymes is their reutilization as biocatalysts for extended periods of time in industrial condition. Due to their interesting magnetic properties, it is possible to recover enzymes from insoluble or larger substrates, even in the presence of solids. As a coin has two sides, magnetic nanoparticles have some drawbacks, such as the enzyme may be inactive by interaction with each other or interfaces. Interactions between soluble enzymes and interfaces of organic solvent drops or gas bubbles have a very negative effect on the operational stability of the soluble enzymes (*21*). Although in our study some activity of enzyme was lost, in fact, this immobilization protocol still showed an improved storage stability of the immobilized pectinase as well as enhanced performance at higher temperatures and over a wider pH range.

Temperature of Reaction Medium. The effect of the temperature profile on the activity of free and immobilized pectinase was investigated in the temperature range of 20−80 °C; the plot of the activity versus temperature of free enzyme and immobilized pectinase is shown in **Figure 6a**. The rate of enzymatic reactions increases with ascending reaction temperature to a certain value in general; however, up to 50 °C the whole reactive system causes protein denaturation and so decreases the reaction rate. It was found that the optimum temperatures for free pectinase were obtained at 50 °C, whereas the optimum temperature of immobilized pectinase was in the range of 50−60 °C, at which the immobilized pectinase retained >95% of its initial activity. Immobilization of the enzyme enhanced the thermal stability of enzyme compared with the free enzyme. These results would be due to stabilization by the covalent bonding between the pectinase molecule and the support Fe_3O_4/SiO_2/PSStNa/chitosan, limiting the conformational changes and movements under various temperatures. Immobilization by covalent attachment to water-insoluble carriers via glutaraldehyde is one of the simplest and gentlest coupling methods in enzyme technology (*22*). When the immobilization is carried out on preactivated supports, the primary amino groups of the enzyme would react with the aldehyde groups that have been introduced by modification of the amino groups of the support (usually with two glutaraldehyde molecules) (*23, 24*). Furthermore, the cross-linkers [2.5% glutaraldehyde (pH 4)] are capable of increasing the conformational rigidity of the enzyme and raising the activation energy of the thermal denaturation reaction (*25*).

pH of Reaction Medium. The effect of pH on the activity of free and immobilized pectinase was assayed; the optimal immobilization conditions selected from these trials were pH values of 2.5−5.0. Typical results are presented in **Figure 6b**. The maximum activity of immobilized enzyme was obtained at pH 3.5, 0.5 unit lower than that of free enzyme (as shown by the dotted horizontal line in **Figure 6b**). Moreover, compared to free enzyme, immobilized enzyme used in this experiment retained >95% activity over a wider pH range of 3.0−4.7. This result can also be attributed to the fact that the microenvironment of the immobilized enzyme on the Fe_3O_4/SiO_2-*g*-PSStNa/chitosan particles might have been buffered and immobilized enzyme was less affected by the acidity of the solution. In

Table 2. Determination of Kinetic Parameters for Free and Immobilized Pectinase at 37 °C

kinetic parameter	free enzyme	immobilized enzyme
K_m (g of pectin mL^{-1})	8.28	10.08
V_{max}[a]	1.17	1.20

[a] $\times 10^{-3}$ g of pectin s^{-1} g of enzyme^{-1} and $\times 10^{-3}$ g of pectin s^{-1} g of particle^{-1} for free and immobilized enzymes, respectively.

addition, upon immobilization the active site becomes more exposed to solvent than in the folded-dissolved pectinase form; hence, proton transfer to the amino acid residues at the active site becomes less hindered. Furthermore, chitosan belongs to the polycationic polymer, so that the pH optimum of the immobilized enzyme on the Fe_3O_4/SiO_2-*g*-PSStNa/chitosan particles shifted slightly in the acidic region.

Storage Stability. Due to storage and application of the immobilized enzyme systems in the physiological environment, the activity of the immobilized pectinase and the storage stability imparted by the support were also examined. The comparative plot is seen in **Figure 6c**, from which we observe that there was a significant decrease in the activity of the immobilized and free enzyme over 30 days, but the amount of desorption and deactivation of the immobilized enzyme is smaller than that of the free enzyme, especially at longer durations. The immobilized enzyme presented >50% of its initial activity over 30 days, whereas free enzyme maintained only <8%. One possible reason for these results of immobilized enzyme is that because the enzyme molecule is attached with a covalent bond to the support matrix, it avoids denaturation of the enzyme molecule for a long period. In addition, it is possible that the enzyme attached to Fe_3O_4/SiO_2-*g*-PSStNa/chitosan by covalent bonding preserves the ternary structure of the enzyme from denaturation.

Kinetic Parameters. The Michaelis constants (K_m) for free and immobilized enzyme were determined through Lineweaver−Burk plot at 37 °C, from which maximal activities (V_{max}) and Michaelis−Menten constants (K_m) values are calculated. K_m and V_{max} calculated from the equations of these plots are summarized in **Table 2**. V_{max} defines the highest possible velocity when all of the enzyme is saturated with substrate; therefore, this parameter reflects the intrinsic characteristics of the immobilized enzyme, but may be affected by diffusional constraints. K_m is defined as the substrate concentration that gives a reaction velocity of $^1/_2V_{max}$. This parameter reflects the effective characteristics of the enzyme and depends upon both partitioning and diffusional effects. K_m and V_{max} calculated from the equations of these plots are summarized in **Table 2**. For pectinase, immobilization hardly affects K_m or V_{max}. The small increase in K_m and decrease in V_{max} are very likely below the experimental error.

LITERATURE CITED

(1) Thakur, B. R.; Singh, R. K.; Handa, A. K. Chemistry and uses of pectin—a review. *Crit. Rev. Food Sci. Nutr.* **1997**, *37*, 47–73.

(2) Willats, W. G. T.; Knox, J. P.; Mikkelsen, J. D. Pectin: new insights into an old polymer are starting to gel. *Trends Food Sci. Technol.* **2006**, *17*, 97–104.

(3) Van Cutsem, P.; Messiaen, J. Cell wall pectins: from immunochemical characterization to biological activity. *Prog. Biotechnol.* **1996**, *14*, 135–149.

(4) Altun, G. D.; Cetinus, S. A. Immobilization of pepsin on chitosan beads. *Food Chem.* **2007**, *100*, 964–971.

(5) Sheldon, R. A. Enzyme immobilization: The quest for optimum performance. *Adv. Synth. Catal.* **2007**, *349* (8−9), 12891307.

(6) Cesar, M.; Jose, M. P.; Gloria, F. L.; Jose, M. G.; Roberto, F. L. Improvement of enzyme activity, stability and via immobilization techniques. *Enzyme Microb. Technol.* **2007**, *40*, 1451–1463.

(7) Dyal, A.; Loos, K.; Noto, M.; Chang, S. W.; Spagnoli, C.; Shafi, K. V. P. M.; et al. Activity of *Candida rugosa* lipase immobilized on *Y*-Fe_2O_3 magnetic nanoparticles. *J. Am. Chem. Soc.* **2003**, *125*, 1684–1685.

(8) Kahraman, M. V.; Bayramoglu, G.; Apohan, N. K.; Güngor, A. α-Amylase immobilization on functionalized glass beads by covalent attachment. *Food Chem.* **2007**, *104*, 1385–1392.

(9) Weng, C. C.; Wei, K. H. Selective distribution of surface-modified TiO_2 nanoparticles in polystyrene-*b*-poly (methyl methacrylate) diblock copolymer. *Chem. Mater.* **2003**, *15*, 2936–41.

(10) Ugelstad, J.; Ellingsen, T.; Berge, A.; Hellgee, O. B. U.S. Patent 4,654,267, 1987.

(11) Wang; Matyjaszewski. XXXX. *XXXX* **XXXX**, *XXX*, xxxx–xxxx.

(12) Kouassi, G. K.; Irudayaraj, J. Magnetic and gold-coated magnetic nanoparticles as a DNA sensor. *Anal. Chem.* **2006**, *78*, 3234–3237.

(13) Li, C. Z.; Benicewicz, B. C. Synthesis of well-defined polymer brushes grafted onto silica nanoparticles via surface reversible addition-fragmentation chain transfer polymerization. *Macromolecules* **2005**, *38*, 5929–5936.

(14) Morinaga, T.; Ohkura, M.; Ohno, K.; Tsujii, Y.; Fukuda, T. Monodisperse silica particles grafted with concentrated oxetane-carrying polymer brushes: their synthesis by surface-initiated atom transfer radical polymerization and use for fabrication of hollow spheres. *Macromolecules* **2007**, *40*, 1159–1164.

(15) Li, D. J.; Jones, G. L.; Dunlap, J. R.; Hua, F. J.; Zhao, B. Thermosensitive hairy hybrid nanoparticles synthesized by surface-initiated atom transfer radical polymerization. *Langmuir* **2006**, *22*, 3344–51.

(16) Zhongli, L.; Yanli, L.; Xiangyu, W. A facile two-step modifying process for preparation of poly (SStNa)-grafted Fe_3O_4/SiO_2 particles. *J. Solid State Chem.* **2008**, *181*, 480–486.

(17) Miller, G. L. Use of dinitrosalicylic acid reagent for determination of reducing sugar. *Anal. Chem.* **1959**, *31*, 426–428.

(18) Bailey, M. J.; Pessa, E. Strain and process for production of polygalacturonase. *Enzyme Microb. Technol.* **1990**, *12*, 266–271.

(19) Kim, J. B.; Grate, J. W. Single-enzyme nanoparticles armored by a nanometer-scale organic/inorganic network. *Nano Lett.* **2003**, *3*, 1219–1222.

(20) Zaitsev, V. S.; Filimonov, I. A.; Presnyakov, J. Physical and chemical properties of magnetite and magnetite-polymer nanoparticles and their colloidal dispersions. *Colloid Interface Sci.* **1999**, *212*, 49.

(21) Lorena, B.; Fernando, L. G.; Aurelio, H.; Noelia, A. M; Manuel, F.; Roberto, F. L.; José, M. G. Prevention of interfacial inactivation of enzymes by coating the enzyme surface with dextran-aldehyde. *J. Biotechnol.* **2004**, *110*, 201–207.

(22) Wine, Y.; Cohen-Hadar, N.; Freeman, A.; Frolow, F. Enzyme stabilization by glutaraldehyde crosslinking of adsorbed proteins on aminated supports. *Biotechnol. Bioeng.* **2007**, *98*, 711–718.

(23) Migneault, I.; Dartiguenave, C.; Bertrand, M. J.; Waldron, K. C. Glutaraldehyde: behavior in aqueous solution, reaction with proteins, and application to enzyme crosslinking. *Biotechniques* **2004**, *37*, 790–802.

(24) Walt, D. R.; Agayn, V. I. The chemistry of enzyme and protein immobilization with glutaraldehyde. *Trends Anal. Chem.* **1994**, *13*, 425–430.

(25) Martinek, K.; Mozaev, V. V.; Berezin, I. V. Stabilization and reactivation of enzymes. In *Enzyme Engineering*; Wingard, L. B., Jr., Berezin, L. V., Klyosov, A. A., Eds.; Plenum Press: New York, 1980; pp 3−54.

Received for review September 18, 2008. Revised manuscript received December 15, 2008. Accepted December 15, 2008.

JF802913M